Coordination Chemistry Reviews 255 (2011) 2530–2541

Contents lists available at ScienceDirect

Coordination Chemistry Reviews

journal homepage: www.elsevier.com/locate/ccr

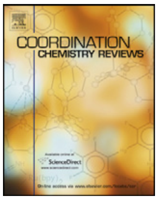

Review

Metal alkynyl complexes as switchable NLO systems☆

Katy A. Green[a], Marie P. Cifuentes[a], Marek Samoc[b,c], Mark G. Humphrey[a,*]

[a] Research School of Chemistry, Australian National University, Canberra, ACT 0200, Australia
[b] Laser Physics Centre, Research School of Physics and Engineering, Australian National University, Canberra, ACT 0200, Australia
[c] Institute of Physical and Theoretical Chemistry, Wroclaw University of Technology, 50-370 Wroclaw, Poland

Contents

1. Introduction 2530
2. Nonlinear optics 2531
  2.1. Materials considerations 2531
  2.2. Theoretical considerations 2531
3. Molecular switches 2532
  3.1. Optical switches 2532
  3.2. Chemical, electrochemical, and magnetic switches 2534
4. Switching NLO properties of metal complexes 2535
  4.1. Optical NLO switching 2536
  4.2. Electrochemical and magnetic switching 2537
5. Metal alkynyl complexes as NLO switches 2538
  5.1. Electrochemical switching 2538
  5.2. Protic switching 2539
  5.3. Multi-stimuli switching 2539
6. Concluding remarks 2540
  Acknowledgements 2540
  References 2540

ARTICLE INFO

Article history:
Received 29 September 2010
Accepted 27 February 2011
Available online 4 March 2011

Keywords:
Organometallic
Nonlinear optics
Molecular switches
Hyperpolarizabilities
Alkynyl complexes

ABSTRACT

Progress in employing metal alkynyl complexes as nonlinear optical (NLO) switchable systems is reviewed. The origin of NLO effects in molecules is summarized, molecular switching stimuli and read-outs are briefly reviewed, and switching NLO properties using other organic, inorganic, and organometallic molecules is also briefly summarized.

1. Introduction

The nonlinear optical (NLO) properties of molecular materials have been of considerable interest since the advent of the laser [1]. Studies of the NLO properties of organometallics commenced ca. twenty-five years ago and, in the interim, sufficient progress has ensued to permit the development of molecular structure–NLO activity relationships [2]. The two classes of organometallics that have been the subject of most scrutiny are ferrocenyl and metal alkynyl complexes, for reasons of facile syntheses, ease of functionalization, oxidative, thermal, and photochemical stability, and

---

Abbreviations: CPD, metacyclophanediene; DHA, dihydroazulenes; DHP, dihydropyrenes; MLCT, metal-to-ligand charge-transfer; NLO, nonlinear optical; SCO, spin crossover; SHG, second-harmonic generation; TTF, tetrathiafulvalene; VHF, vinylheptafulvenes.

☆ Contribution to the Special Issue "Controlling Photophysical Properties of Metal Complexes: Toward Molecular Photonics".

* Corresponding author. Tel.: +61 2 61252927; fax: +61 2 61250750.
E-mail address: Mark.Humphrey@anu.edu.au (M.G. Humphrey).

0010-8545/$ – see front matter © 2011 Elsevier B.V. All rights reserved.
doi:10.1016/j.ccr.2011.02.021

significant NLO activity. Several years ago, we reviewed the NLO properties of metal alkynyl complexes, and concluded "switching the quadratic and cubic nonlinearity is an area that is likely to undergo further developments in the near future" [3]. In this review, and following brief overviews of NLO materials, the theory of nonlinear optics, and molecular switching stimuli and read-outs, we summarize the progress thus far in NLO switching employing metal alkynyl complexes. While the present work is intended to be "stand-alone", the coverage of metal alkynyl complexes is restricted to those for which the possibility of NLO switching has been assayed; the reader is directed to our earlier review [3] for a more broad-ranging treatment of metal alkynyl complex structure–NLO activity relationships.

2. Nonlinear optics

2.1. Materials considerations

NLO effects arise when intense electromagnetic fields, typically those present in a laser beam, interact with matter. The ability of NLO materials to generate new field components (differing in amplitude, phase, frequency, path, polarization, etc.) is of enormous technological importance in optical devices, with applications in data storage, telecommunications, switching, image processing, computing, biological imaging, and nanofabrication. These applications have generated a need for materials with exceptional NLO properties and satisfactory materials properties (processing, stability, etc.).

Materials currently employed for their NLO properties are mostly inorganic salts such as $LiNbO_3$ and KH_2PO_4 that are used in frequency mixing and electro-optic modulation applications, which rely on second-order NLO properties, and glasses such as silica, chalcogenides and fluorides used for third-order NLO applications. Inorganic salts have desirable properties for materials applications, including a large transparency range, high optical damage threshold and the fact that they can be grown as large crystals. However, they have restricted structural diversity and can be difficult to fabricate. In these materials, the purely electronic NLO effects, which are effectively instantaneous, are often accompanied by slower (e.g. nanosecond time scale) responses, and the high values of the dielectric constant of some of them impose limitations on the speed of devices employing the electro-optic effect. Semiconductors such as gallium arsenide and cadmium sulfide, particularly species with reduced dimensions (quantum wells, quantum wires, and quantum dots), are attractive because of sizeable third-order NLO effects that arise from resonant interactions such as saturable absorption. Materials using resonant NLO effects suffer, however, from limitations due to strong absorption losses and a relatively slow response time. Some semiconductors such as $Al_xGa_{1-x}As$ have reasonably high non-resonant nonlinearities, but there is limited architectural flexibility in these materials.

Organic molecules have much greater design flexibility than inorganic compounds, which allows for the fine-tuning of NLO responses, and they can be much cheaper and easier to fabricate. The NLO effects in organic molecules are usually electronic in nature, which leads to fast nonlinear response. The architectural flexibility allows for precise molecular design and the determination of structure–property relationships. Low-lying electronic transitions in the UV–visible region improve the NLO efficiencies of organic systems, but lead to a disadvantageous trade-off between nonlinear efficiency and optical transparency. Another disadvantage of organic compounds is that they often have lower thermal and photochemical stability than inorganic compounds. Organic chromophores have, however, a definite advantage as efficient nonlinear absorbers [1e].

Organometallic complexes can possess large NLO responses, fast response times, ease of fabrication and integration into composites, as well as having greater design flexibility than purely organic compounds. Organometallic complexes can be formed using a wide range of metals with different oxidation states, ligands and geometries. The metal may act variously as a donor or acceptor group, and mixed-metal systems are also readily accessible. Organic fragments that would otherwise be too unstable to examine may be stabilized by complexation to a metal (e.g. carbenes). For all of the aforementioned reasons, organometallics have attracted significant attention as possible NLO materials.

2.2. Theoretical considerations

For materials composed of organic or organometallic molecules, it is convenient to consider NLO interactions at the molecular level. When a local electric field $\mathbf{E}_{loc}$ acts upon a molecule it distorts the molecule's electron density distribution $\rho(\mathbf{r})$. When the electric field is weak (in comparison to the internal electric fields of a molecule), the dipole induced by the field is in a linear relationship to the field strength. However, if the field is strong then the relationship becomes nonlinear. This dependence of the dipole moment on the electric field is usually represented as a power series:

$$\boldsymbol{\mu} = \boldsymbol{\mu}_0 + \boldsymbol{\alpha}\mathbf{E}_{loc} + \boldsymbol{\beta}\mathbf{E}_{loc}\mathbf{E}_{loc} + \boldsymbol{\gamma}\mathbf{E}_{loc}\mathbf{E}_{loc}\mathbf{E}_{loc} + \cdots \tag{1}$$

where $\boldsymbol{\mu}_0$ is the static dipole moment, $\boldsymbol{\alpha}$ is the linear polarizability, $\boldsymbol{\beta}$ is the second-order polarizability, and $\boldsymbol{\gamma}$ is the third-order polarizability. The second-order polarizability is often referred to as the first hyperpolarizability or quadratic hyperpolarizability and, similarly, the third-order polarizability is the second hyperpolarizability or cubic hyperpolarizability. As $\boldsymbol{\mu}$ and $\mathbf{E}_{loc}$ are vectors, the polarizabilities are tensors of appropriate ranks: $\boldsymbol{\alpha}$ is a second-rank tensor (with 9 components), $\boldsymbol{\beta}$ is a third-rank tensor (27 components), and $\boldsymbol{\gamma}$ is a fourth-rank tensor (81 components). Fortunately, many of the tensor components of $\boldsymbol{\alpha}$, $\boldsymbol{\beta}$, and $\boldsymbol{\gamma}$ are equivalent by various symmetry rules or equal to zero [4]. Macroscopic parameters describing the NLO properties of a material built of NLO chromophores are denoted $\chi^{(2)}$ and $\chi^{(3)}$ for the quadratic and cubic susceptibility tensors, respectively. The components of the $\chi^{(2)}$ and $\chi^{(3)}$ tensors can be obtained by appropriate summing of the $\boldsymbol{\beta}$ and $\boldsymbol{\gamma}$ tensor components, transformed taking into account the orientations of the individual molecules. This complicated procedure is simplified considerably with isotropic materials (e.g. solutions or glasses) or systems with relatively high symmetry (e.g. electric field-poled polymers), for which averaging procedures can be used to describe an NLO response of a statistically disordered assembly of NLO chromophores. In particular, in an isotropic material composed of randomly oriented molecules, all tensor components of $\chi^{(2)}$ have to be equal to zero, while the diagonal components of $\chi^{(3)}$ can be calculated as:

$$\chi^{(3)}_{IIII} = NL^4\langle\gamma\rangle = NL^4\frac{1}{5}(\gamma_{1111} + \gamma_{2222} + \gamma_{3333} + 2\gamma_{1122} + 2\gamma_{1133} + 2\gamma_{2233}) \tag{2}$$

where N is the concentration of molecules, L is the local field factor, often approximated as $(n^2+2)/3$, n being the refractive index, and $\langle\gamma\rangle$ is the orientationally averaged cubic hyperpolarizability.

The electric field of a light wave can be expressed as:

$$E(t) = E_0\,\cos(\omega t) = \frac{E_0}{2}[\exp(i\omega t) + \exp(-i\omega t)] \tag{3}$$

Substituting this into Eq. (1), one obtains (neglecting the vector and tensor character of the variables):

$$\begin{aligned}\mu(t) &= \mu_0 + \alpha E_0 \cos(\omega t) + \beta E_0^2 \cos^2(\omega t) + \gamma E_0^3 \cos^3(\omega t) + \cdots \\ &= \mu_0 + \frac{1}{2}\alpha E_0 \exp(i\omega t) + \frac{1}{2}\beta E_0^2 + \frac{1}{4}\beta E_0^2 \exp(2i\omega t) \\ &\quad + \frac{3}{8}\gamma E_0^3 \exp(i\omega t) \\ &\quad + \frac{1}{8}\gamma E_0^3 \exp(3i\omega t) + \text{c.c.} + \cdots\end{aligned} \tag{4}$$

where c.c. denotes complex conjugate terms. From the above equation it is clear that the presence of higher order terms leads to generation of new frequencies of molecular dipole oscillation. It should be noted that the 'β term' in Eq. (1) causes the appearance of frequency doubling (2ω) (second-harmonic generation) while the 'γ term' yields frequency tripling (3ω) (third-harmonic generation). In addition, the second-order term generates a time-independent contribution to the dipole (called 'optical rectification') and there is also a cubic term due to γ, oscillating at the frequency ω, which is responsible for nonlinear refraction (intensity-dependent refractive index).

Eq. (4) describes the behavior of the induced dipole if the frequency of the optical field is far from any material resonances. If this is not the case, one needs to take the damping of the dipole oscillation into account, which results in a change in amplitude and a phase lag with respect to the field. This is accomplished by considering Fourier components of the field and the dipole oscillation at particular frequencies. To account for the damping, one needs to treat the linear and higher order frequency-dependent polarizabilities as being complex (that is, composed of real and imaginary parts, both being frequency dependent). The linear Fourier component of the induced dipole is then written as:

$$\Delta\mu^{(1)}(\omega) = \alpha(\omega)E(\omega) \tag{5}$$

where $\Delta\mu^{(1)}(\omega)$ is the linear component of the oscillation of the dipole at the frequency ω, $E(\omega)$ is the Fourier amplitude of the field at that frequency, and $\alpha(\omega)$ is the linear polarizability, which is a complex quantity in which the real part is responsible for refractive properties of matter and the imaginary part is related to the absorption coefficient. The frequency dependence of the higher polarizabilities may be written as:

$$\Delta\mu^{(2)}(\omega_3) = \beta(-\omega_3; \omega_1, \omega_2)E(\omega_1)E(\omega_2) \tag{6}$$

$$\Delta\mu^{(3)}(\omega_4) = \gamma(-\omega_4; \omega_1, \omega_2, \omega_3)E(\omega_1)E(\omega_2)E(\omega_3) \tag{7}$$

The nonlinear polarizabilities corresponding to different combinations of input frequencies are different, and one therefore needs to specify all the input frequencies explicitly, together with a sign denoting how a given frequency enters the combination giving the output frequency. For example, the nonlinear polarizability responsible for the electro-optic effect is specified as $\beta(-\omega; \omega, 0)$ while that for the second-harmonic generation process is $\beta(-2\omega; \omega, \omega)$. The important case of a degenerate cubic hyperpolarizability (responsible for nonlinear refraction and nonlinear absorption) at a frequency ω is denoted as $\gamma(-\omega; \omega, -\omega, \omega)$.

Strong dispersion of the real parts of the polarizabilities and large values of the imaginary parts are expected when input frequencies or the output frequency (or, in some cases, certain combinations of the frequencies) approach resonance frequencies of the molecule. In particular, for the degenerate case of the cubic nonlinearity described by $\gamma(-\omega; \omega, -\omega, \omega)$, the imaginary part of γ, γ_{imag}, is related to nonlinear absorption, often defined as two-photon absorption and expected to be significant for 2ω in the vicinity of molecular two-photon-allowed transitions. It should be noted that two-photon absorption of molecules is often quantified using the so-called two-photon absorption cross-section σ_2, which is thus related to γ_{imag}. The significant frequency dependence of nonlinearity implicit in the foregoing discussion suggests that NLO spectral dependence studies are mandatory, a requirement that was not satisfied in earlier studies due to the lack of appropriate wavelength-tuneable lasers, but which is now being addressed.

3. Molecular switches

Molecular switches are molecules that are reversibly switchable between at least two forms that have different "readable" properties (e.g. optical, electrical, magnetic), and are stable in these forms for at least as long as the measurement time for the readout. Although the change in any readable property can form the basis for a switch, the majority of switches involve changes in the optical and/or the electrical properties of the compound [5]. Light is also the most common stimulus used to bring about such changes. Other common stimuli include electricity, pH control, and magnetism [6]. The field of molecular switches is large and rapidly expanding [7], and a brief summary of the major types of molecular switches and their characteristic properties follows, of interest *inter alia* because these switching species can be functionalized and incorporated into metal complexes.

3.1. Optical switches

Optically switchable compounds are of potential interest in the growing areas of molecular electronics and optical communication. The main types of photochemical switches involve either a *cis–trans* photoisomerization or a photoinduced ring-closure/ring-opening reaction. Azobenzenes and overcrowded alkenes can undergo a photo-induced *cis–trans* isomerization [6c,8], often with a distinct change in their optical absorption in the visible region; most of these switches are not thermally stable and revert to the ground state at room temperature in the dark. Rhodopsin and bacteriorhodopsin [6d,9] are biological proteins used in vision and energy generation, respectively, that undergo *cis–trans* photoisomerization. Bacteriorhodopsin has seven α-helical bundles encasing a retinal residue; these bundles control the environment, allowing only an all-*trans* to 13-*cis* isomerization.

Recently, there has been much interest in photochemical ring-closure or ring-opening switches. These switches may differ in the wavelength of light required to switch the molecule, the physical properties of the two forms, the thermal and chemical stability of the forms, and the fatigue resistance of the switch. There have also been reports of switches combining more than one type of ring-closure unit, allowing access to more states. Dihydroazulenes (DHA) can be converted to vinylheptafulvenes (VHF) on exposure to light (Fig. 1(a)) [10]. The strongly coloured VHF form is then converted back to the DHA form at room temperature in the dark. Changing the R group affects the time taken to convert and the formation of by-products [11]. Spiropyrans and the related spiroxazines [6b,12] undergo a ring-opening reaction on exposure to UV light, cleaving a C–O bond (Fig. 1(b) and (c)). The ring-opened form converts back to the closed form at room temperature in the dark, a process that can be accelerated by a different wavelength of light. These switches have been studied for potential use in a three-dimensional optical memory [13] and as an optical control of protein activity by covalently bonding the switching unit to the protein [14]. Naphthopyrans [15] are ring-closure switches that operate via a C–O bond formation (Fig. 1(d)). These compounds undergo a ring-closure reaction when exposed to one wavelength of light, and are subsequently opened by exposure at another wavelength, or at room temperature in the dark. Naphthopyrans are currently in commercial use in plastic ophthalmic lenses [16].

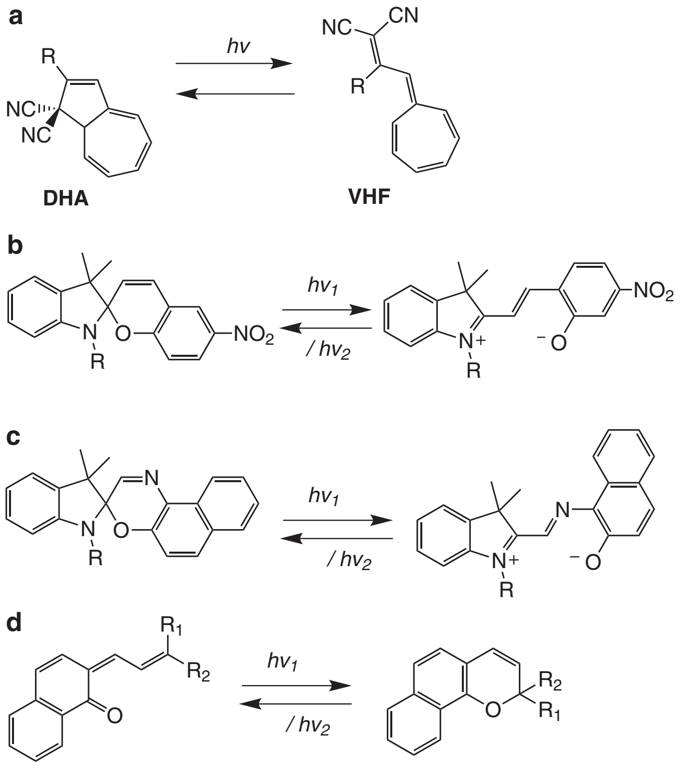

Fig. 1. (a) The photo-induced ring-opening of dihydroazulenes (DHA) [10]. (b) The photo-induced ring-opening of spiropyrans [6b]. (c) The photo-induced ring-opening of spirooxazines [6b]. (d). The photo-induced ring-closure of naphthopyrans [15].

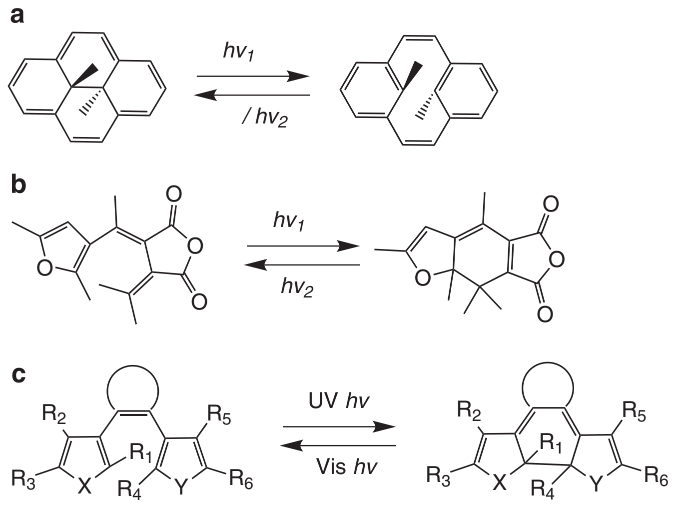

Fig. 2. (a) The photo-induced ring-opening of dihydropyrenes [17]. (b) The photo-induced ring-closure of fulgides [6f]. (c) The photo-induced ring-closure of diarylethenes [6e].

Dihydropyrenes (DHP) [17] are generally ring-opening switches (Fig. 2(a)); however, with some substituents, the ring-open form (metacyclophanediene, CPD), is more stable. The compound slowly reverts to the more stable form in the dark, or can be rapidly switched with light. The ring structure of the open CPD form means that there is less molecular motion involved in the switching than with most other ring-closure/opening molecules. The confined structure also limits the number of possible side reactions, making it more stable. Fulgides (Fig. 2(b)), fulgimides and related compounds undergo a ring-closure reaction, fusing the side of an aromatic ring to form a 6-membered ring, and in the process losing the aromaticity [6f]. Although the original fulgides were thermally reversible, their structure has since been modified to form a variety of thermally irreversible fulgides and related compounds. Modifications have also been made to improve other desirable switch properties such as thermal stability, fatigue resistance, and high efficiency of the photoreactions. These improvements have made fulgides and related compounds of great interest in optical mem-

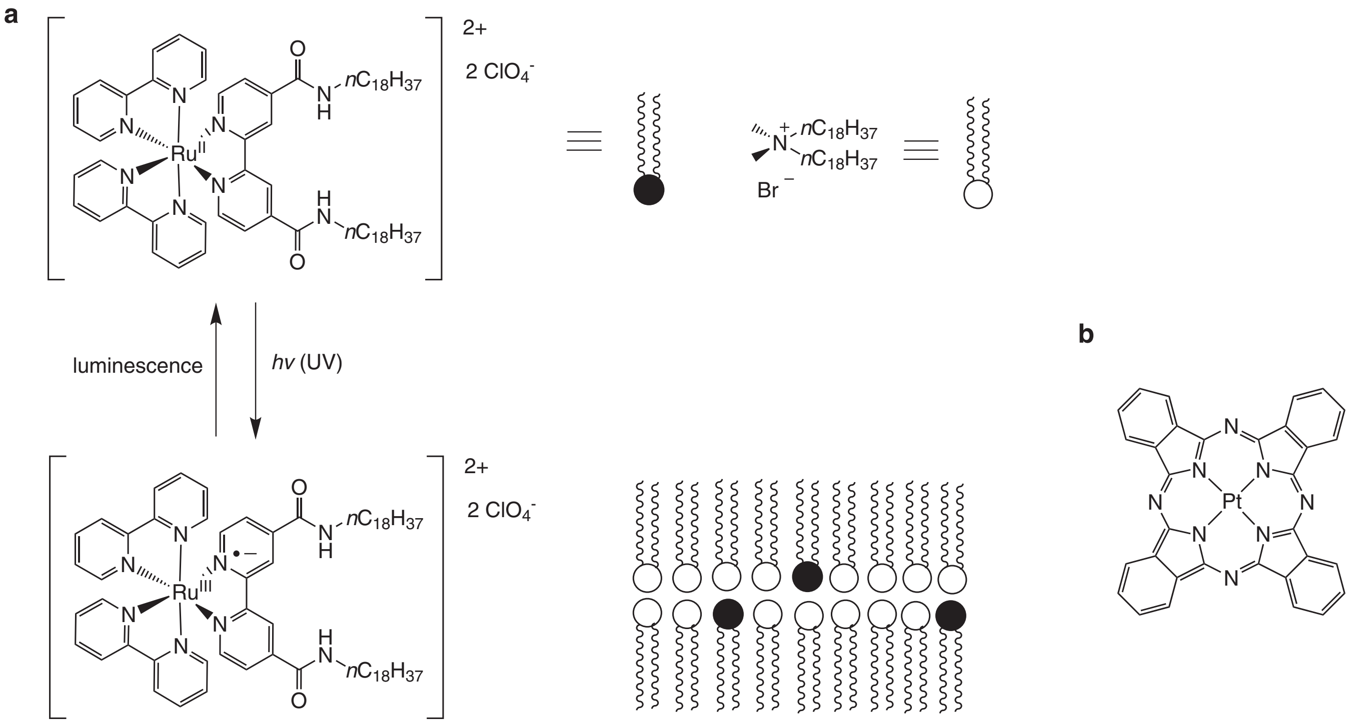

Fig. 3. (a) A ruthenium-containing Langmuir–Blodgett film optical switch [21]. (b) A platinum phthalocyanine complex employed as an optical switch [22].

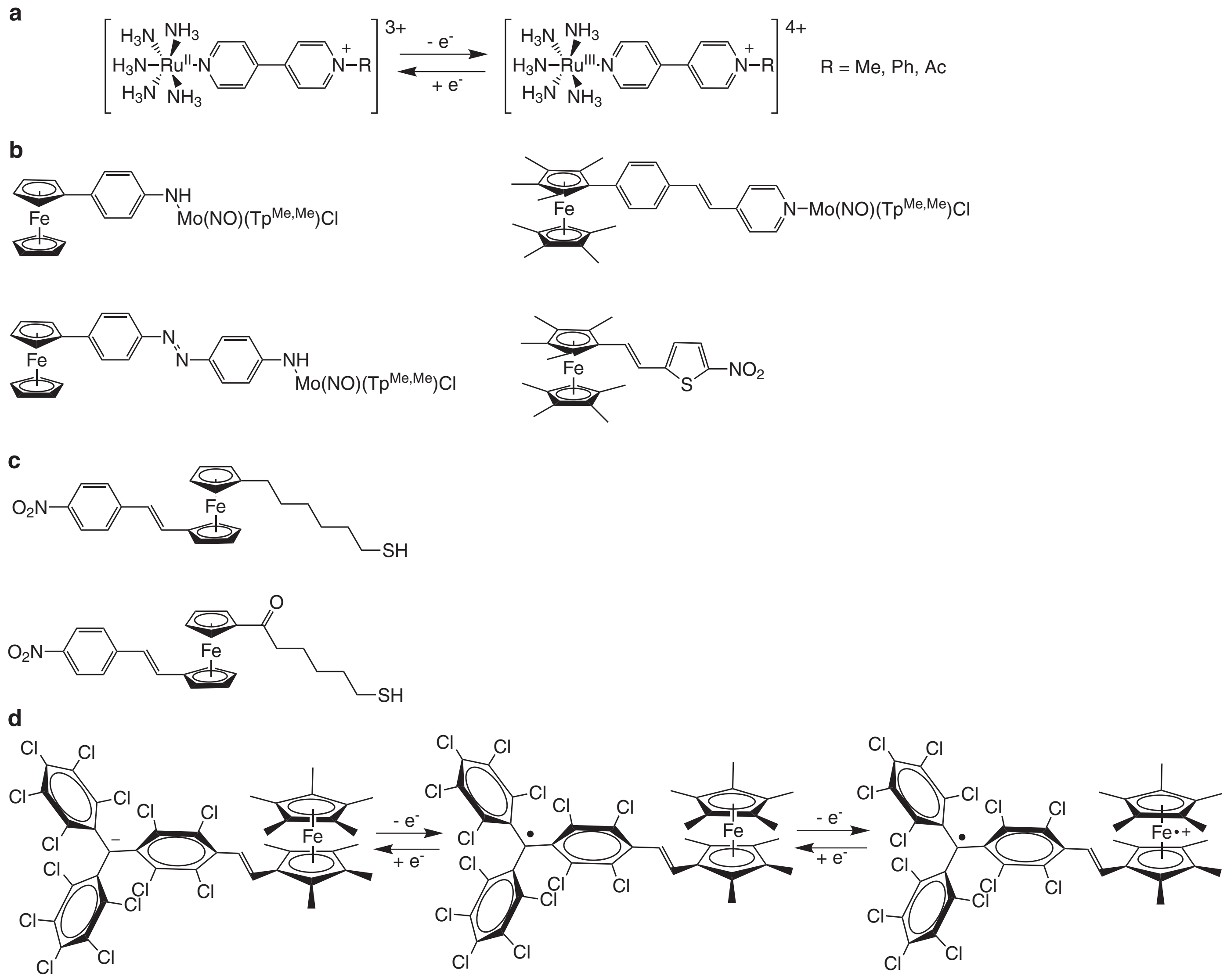

Fig. 4. (a) Ruthenium ammine complexes used as redox switches [24]. (b) Ferrocene-based redox switches ($T_p{}^{Me,Me}$ = tris(3,5-dimethylpyrazolyl)borate) [26]. (c) Surface-supported ferrocene-based redox switches [28]. (d) A three-state ferrocene-based redox switch [29].

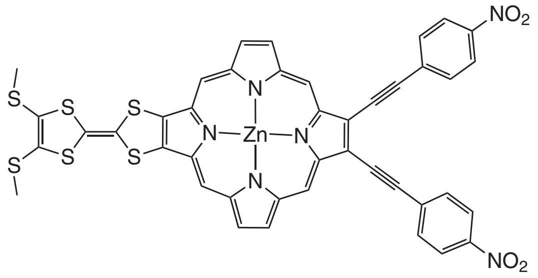

Fig. 5. A porphyrin-tetrathiafulvalene redox switch [31].

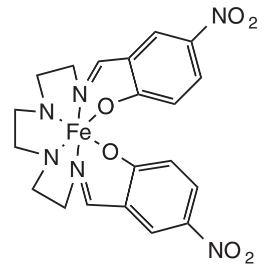

Fig. 6. A Schiff base magnetic spin crossover switch [34].

ory applications. The final important photochemical switches are diarylethenes, which undergo a reversible ring-closure reaction in which both forms are thermally stable and are inter-converted by different wavelengths of light (Fig. 2(c)) [6e,18]. The ring-closure creates a conjugated pathway through the molecule, resulting in a strongly coloured closed form and some interesting optical and electronic properties. The most common form of these switches has two thiophenes as the heteroaryl rings and perfluorocyclopentene, maleic anhydride or maleimides as the bridge. These compounds have high fatigue resistance.

3.2. Chemical, electrochemical, and magnetic switches

Chemical switches have attracted significant interest due to their potential applications as sensors for a varied of neutral and charged compounds [19]. The structure of such compounds gen-

Table 1
Switching of molecular NLO properties by oxidation/reduction at a single wavelength (Hyper-Rayleigh scattering, 1064 nm, electric field-induced second-harmonic generation, 1907 nm, and Z-scan, 800 nm).

Complex	λ (nm)	β (10^{-30} esu)	β_0 (10^{-30} esu)	Stimulus	Technique, solvent	Ref.
$[1,3\text{-}C_6H_4\{(C{\equiv}C)Fe(dppe)(\eta^5\text{-}C_5Me_5)\}_2]$	349	210	98		HRS, CH_2Cl_2	[35]
$[1,3\text{-}C_6H_4\{(C{\equiv}C)Fe(dppe)(\eta^5\text{-}C_5Me_5)\}_2]PF_6$	650	150	21	Redox	HRS, CH_2Cl_2	[35]
$[1,3\text{-}C_6H_4\{(C{\equiv}C)Fe(dppe)(\eta^5\text{-}C_5Me_5)\}_2](PF_6)_2$	662	200	30	Redox	HRS, CH_2Cl_2	[35]
$[1,3,5\text{-}C_6H_3\{(C{\equiv}C)Fe(dppe)(\eta^5\text{-}C_5Me_5)\}_3]$	351	175	87		HRS, CH_2Cl_2	[35]
$[1,3,5\text{-}C_6H_3\{(C{\equiv}C)Fe(dppe)(\eta^5\text{-}C_5Me_5)\}_3]PF_6$	710	190	35	Redox	HRS, CH_2Cl_2	[35]
$[1,3,5\text{-}C_6H_3\{(C{\equiv}C)Fe(dppe)(\eta^5\text{-}C_5Me_5)\}_3](PF_6)_2$	688	170	29	Redox	HRS, CH_2Cl_2	[35]
$[1,3,5\text{-}C_6H_3\{(C{\equiv}C)Fe(dppe)(\eta^5\text{-}C_5Me_5)\}_3](PF_6)_3$	662	53	8	Redox	HRS, CH_2Cl_2	[35]
$[1,4\text{-}C_6H_4\{(C{\equiv}C)Fe(dppe)(\eta^5\text{-}C_5Me_5)\}_2]$	413	180	60		HRS, CH_2Cl_2	[35]
$[1,4\text{-}C_6H_4\{(C{\equiv}C)Fe(dppe)(\eta^5\text{-}C_5Me_5)\}_2]PF_6$	702	400	72	Redox	HRS, CH_2Cl_2	[35]
$[1,4\text{-}C_6H_4\{(C{\equiv}C)Fe(dppe)(\eta^5\text{-}C_5Me_5)\}_2](PF_6)_2$	702	200	36	Redox	HRS, CH_2Cl_2	[35]
$[Fe(C{\equiv}CC_6H_4\text{-}4\text{-}NO_2)(dppe)(\eta^5\text{-}C_5Me_5)\}_2]$	595	168.9	93.0		EFISH, CH_2Cl_2	[36]
$[Fe(C{\equiv}CC_6H_4\text{-}4\text{-}NO_2)(dppe)(\eta^5\text{-}C_5Me_5)\}_2]PF_6$	650	0.04	>0.02	Redox	EFISH, $CHCl_3$	[36]
$[Fe(C{\equiv}CC_6H_4\text{-}4\text{-}CN)(dppe)(\eta^5\text{-}C_5Me_5)\}_2]$	445	69.8	51.0		EFISH, CH_2Cl_2	[36]
$[Fe(C{\equiv}CC_6H_4\text{-}4\text{-}CN)(dppe)(\eta^5\text{-}C_5Me_5)\}_2]PF_6$	652	−1.8	−0.8	Redox	EFISH, $CHCl_3$	[36]
$[Fe(C{\equiv}CPh)(dppe)(\eta^5\text{-}C_5Me_5)\}_2]$	350	54.2	45.3		EFISH, CH_2Cl_2	[36]
$[Fe(C{\equiv}CPh)(dppe)(\eta^5\text{-}C_5Me_5)\}_2]PF_6$	662	−0.5	−0.2	Redox	EFISH, $CHCl_3$	[36]
$[Fe(C{\equiv}CC_6H_4\text{-}4\text{-}OMe)(dppe)(\eta^5\text{-}C_5Me_5)]$	333	10.9	9.2		EFISH, CH_2Cl_2	[36]
$[Fe(C{\equiv}CC_6H_4\text{-}4\text{-}OMe)(dppe)(\eta^5\text{-}C_5Me_5)]PF_6$	718	−18.8	−6.9	Redox	EFISH, $CHCl_3$	[36]
$[Fe(C{\equiv}CC_6H_4\text{-}4\text{-}NH_2)(dppe)(\eta^5\text{-}C_5Me_5)]$	322	17.8	15.3		EFISH, CH_2Cl_2	[36]
$[Fe(C{\equiv}CC_6H_4\text{-}4\text{-}NH_2)(dppe)(\eta^5\text{-}C_5Me_5)]PF_6$	789	−22.0	−5.7	Redox	EFISH, $CHCl_3$	[36]

Complex	λ (nm)	γ_{real} (10^{-36} esu)	γ_{imag} (10^{-36} esu)	$\lvert\gamma\rvert$ (10^{-36} esu)	Stimulus	Z-scan, solvent	Ref.
trans-$[Ru(C{\equiv}CPh)Cl(dppm)_2]$	318	<300	<200	<300		CH_2Cl_2	[37,38]
trans-$[Ru(C{\equiv}CPh)Cl(dppm)_2]^+$	833	1300 ± 500	−2200 ± 1000	2600 ± 1000	Electrochemical	CH_2Cl_2	[37,38]
trans-$[Ru(C{\equiv}CC_6H_4\text{-}4\text{-}C{\equiv}CPh)Cl(dppe)_2]$	388	−100 ± 100	450 ± 200	460 ± 200		CH_2Cl_2	[37,38]
trans-$[Ru(C{\equiv}CC_6H_4\text{-}4\text{-}C{\equiv}CPh)Cl(dppe)_2]^+$	893	2900 ± 1000	−1200 ± 600	3100 ± 1000	Electrochemical	CH_2Cl_2	[37,38]
$[1,3,5\text{-}[$*trans*-$[RuCl(dppe)2(C{\equiv}CC6H4C{\equiv}C)]_3(C_6H_3)]$	413	−330 ± 100	2200 ± 500	2200 ± 600		CH_2Cl_2	[37,40]
$[1,3,5\text{-}\{$*trans*-$RuCl(dppe)2(C{\equiv}CC6H4C{\equiv}C)\}_3(C_6H_3)]3+$	893	13,500 ± 3000	−4700 ± 500	14,000 ± 3000	Electrochemical	CH_2Cl_2	[37,40]

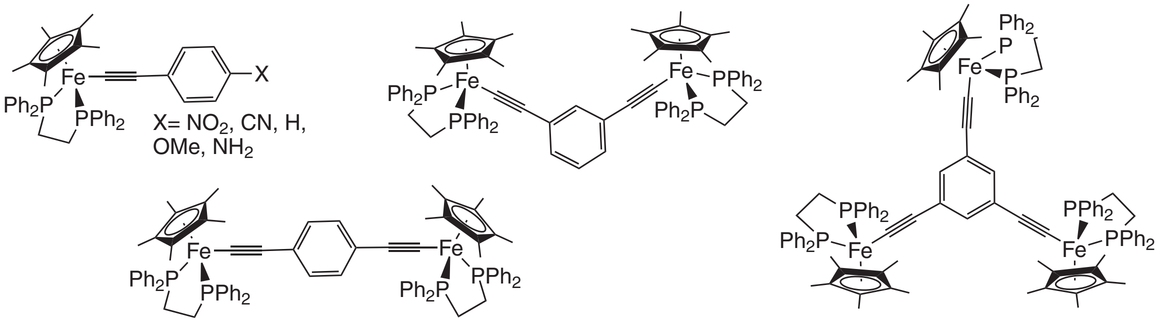

Fig. 7. Iron alkynyl complex switches [35,36].

erally involves a 'detection' part, which should selectively bind to the desired chemical, a linker, which must allow communication between the detector and the reporter, and a 'reporter' section, which should have at least one readable property that is changed on binding with the detector. The readout from the reporter may be optical, electronic, magnetic, or chemical, with fluorescence being one of the most common outputs. The simplest chemical switch, protonation/deprotonation, has been employed to switch nonlinearity in several organic systems (e.g. dimethylamino-functionalized azafulleroids [20]).

Electrochemical switches are of great interest for information processing. Most electrochemical switches involve the redox switching of a metal centre that causes changes in the optical properties or the molecular geometry. As well as the redox switching of small molecules, there has also been much interest recently in the electronic switching of macromolecular assemblies, for which a change in the oxidation state of a metal centre may result in large movements within the assembly.

Although magnets have been in use for a long time for information storage and electronic devices, there are relatively few molecular magnetic switches. The majority of magnetic switches involve spin crossover (SCO) materials [7b]. Many SCO materials, however, use light rather than a magnetic field to switch the magnetic properties.

4. Switching NLO properties of metal complexes

The molecule-based switching of nonlinear optical properties is of great interest in the growing fields of optoelectronics and photonics. The NLO properties of a variety of organic optical switches, such as the azobenzenes, bacteriorhodopsin, and dithienylethenes described above, have been investigated [6a,b,f].

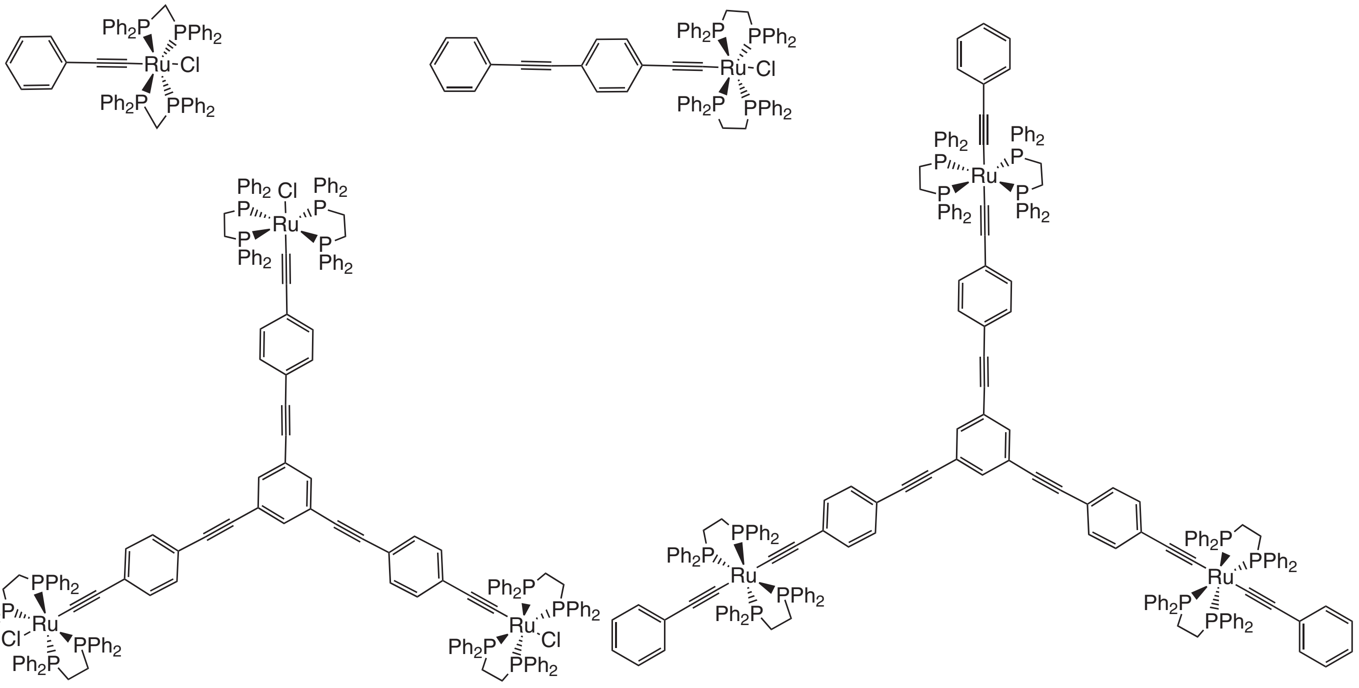

Fig. 8. Ruthenium alkynyl-based redox switches [37–40].

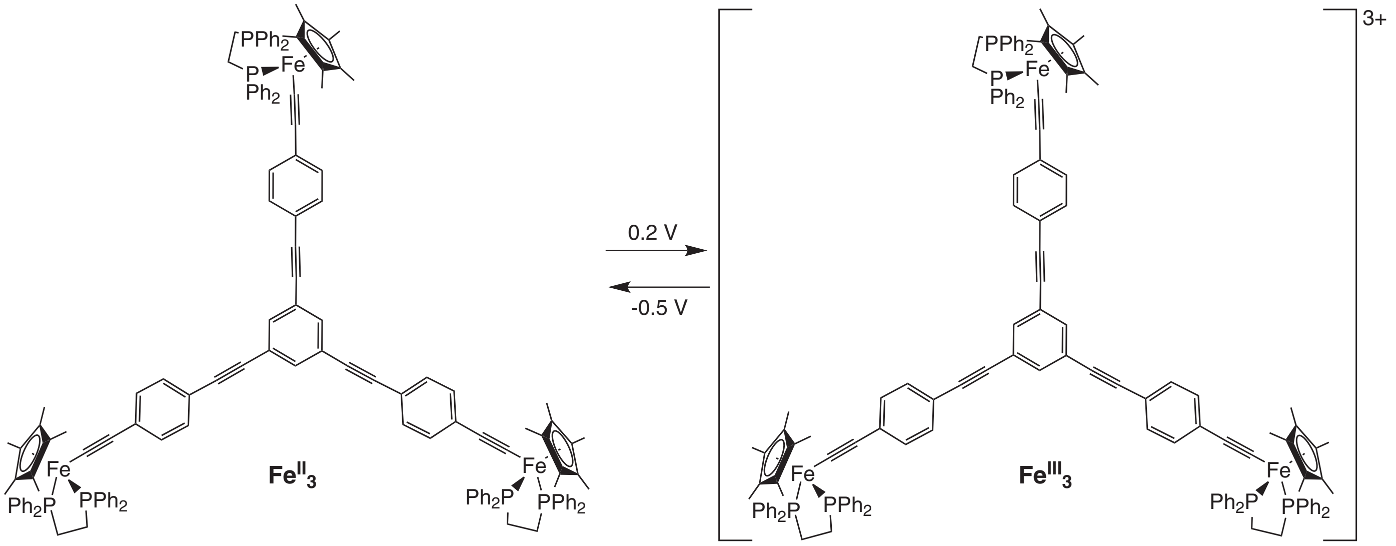

Fig. 9. A triiron alkynyl redox switch. Fe^{II}_3 λ_{max} 460 nm, γ_{real} $-3300 \pm 800 \times 10^{-36}$ esu, γ_{imag} $2800 \pm 700 \times 10^{-36}$ esu, $|\gamma|$ $4300 \pm 1100 \times 10^{-36}$ esu; Fe^{III}_3 λ_{max} 1864 nm, γ_{real} $-2000 \pm 1000 \times 10^{-36}$ esu, γ_{imag} $-3300 \pm 1000 \times 10^{-36}$ esu, $|\gamma|$ $3900 \pm 1400 \times 10^{-36}$ esu (Z-scan, 695 nm, thf solvent) [41].

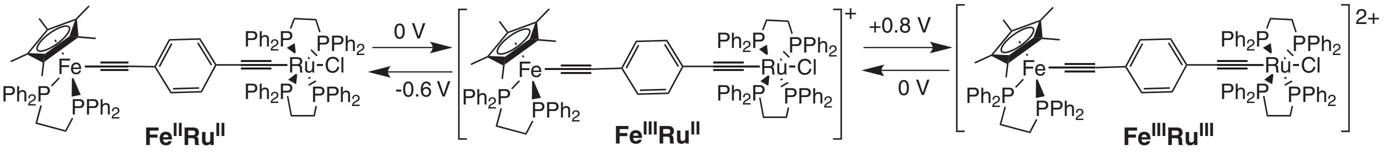

Fig. 10. A ruthenium–iron alkynyl three-state redox switch. $Fe^{II}Ru^{II}$ λ_{max} 378 nm, $\gamma_{real} < 100 \times 10^{-36}$ esu, $\gamma_{imag} < 100 \times 10^{-36}$ esu, $|\gamma|$ ca. 0 esu; $Fe^{III}Ru^{II}$ λ_{max} 1124 nm, γ_{real} $-450 \pm 100 \times 10^{-36}$ esu, γ_{imag} $1600 \pm 200 \times 10^{-36}$ esu, $|\gamma|$ $1700 \pm 250 \times 10^{-36}$ esu; $Fe^{III}Ru^{III}$ λ_{max} 914 nm, $\gamma_{real} < 300 \times 10^{-36}$ esu, γ_{imag} $-970 \pm 200 \times 10^{-36}$ esu, $|\gamma|$ $1000 \pm 300 \times 10^{-36}$ esu (Z-scan, 790 nm, CH_2Cl_2 solvent) [42].

While metal-containing molecules often have larger NLO responses than analogous organic molecules, and also offer the possibility of redox switching, relatively few examples of metal-containing molecular NLO switches exist.

4.1. Optical NLO switching

The first switching of the NLO properties of a metal-containing compound was reported in 1992 [21]. A *tris*-bipyridine ruthenium

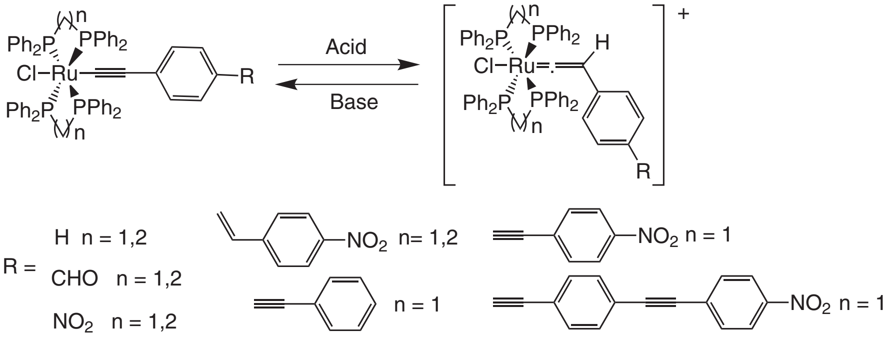

Fig. 11. Protically switchable ruthenium alkynyl complexes [43].

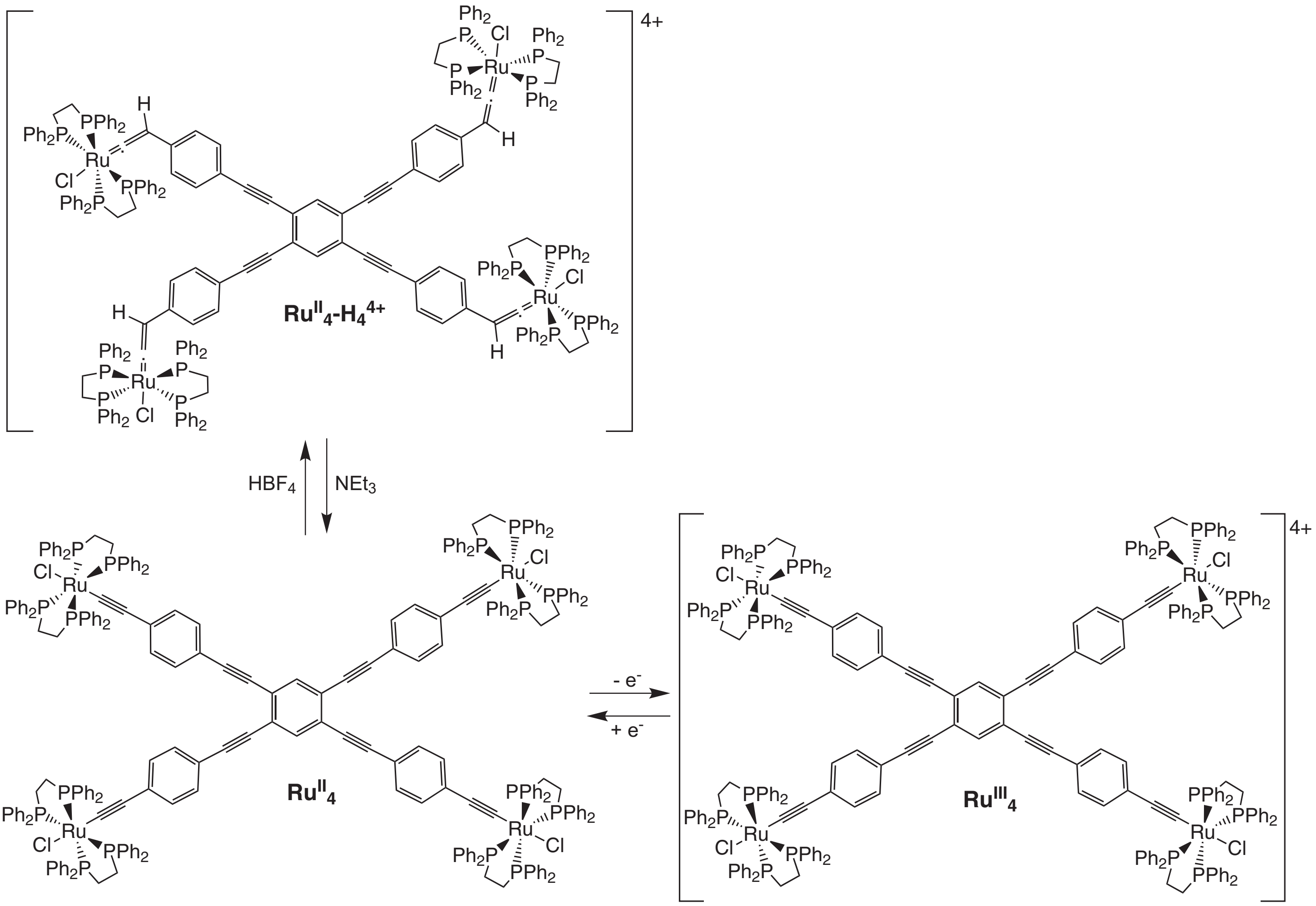

Fig. 12. A ruthenium alkynyl redox and protic switch [44].

derivative was incorporated into a Langmuir–Blodgett (LB) film (Fig. 3(a)), and its second-harmonic generation (SHG) response from irradiation by a 590 nm laser was reduced by 30% following irradiation of the film by 378 nm light; similar results were seen with a 1064 nm laser and 355 nm irradiation. The switching effect results from a metal-to-ligand charge-transfer (MLCT) excitation. Cubic NLO properties have also been switched. Excitation of the platinum phthalocyanine complex shown in Fig. 3(b) with a 514 nm laser beam results in the population of a triplet state which has high absorption at the probe wavelength of 632 nm, resulting in a one-third increase in nonlinear absorption [22].

4.2. Electrochemical and magnetic switching

In 1995, Prasad's group reported the modification of NLO properties by the electrochemical doping of a conducting polymer [23]. The first redox switching of NLO properties in a metal complex was reported in 1999 [24]. Oxidation/reduction reactions on the series of ruthenium ammine complexes shown in Fig. 4(a) were carried out chemically using 1:1 30% aqueous H_2O_2/2 M HCl and 62% hydrazine hydrate, respectively, the oxidized forms having effectively no second-order NLO response in contrast to the Ru^{II} forms. Coe and co-workers have recently incorporated a related ruthenium ammine complex, with a long alkyl chain in the R posi-

Table 2
Switching of molecular NLO properties by protonation/deprotonation at a single wavelength (Hyper-Rayleigh Scattering, 1064 nm, and Z-scan, 800 nm, thf solvent) [43].

Complex	λ (nm)	β (10^{-30} esu)	β_0 (10^{-30} esu)	γ_{real} (10^{-36} esu)	γ_{imag} (10^{-36} esu)	$\lvert\gamma\rvert$ (10^{-36} esu)
trans-[Ru(C≡CPh)Cl(dppm)$_2$]	308	20	12	<120	0	<120
trans-[Ru(C=CHPh)Cl(dppm)$_2$]PF$_6$	320	24	16	<440	<50	<440
trans-[Ru(C≡CPh)Cl(dppe)$_2$]	319	6	3	−170 ± 40[a]	71 ± 20[a]	180 ± 45[a]
trans-[Ru(C=CHPh)Cl(dppe)$_2$]PF$_6$	317	Scatters	Scatters	380 ± 400	<50	380 ± 400
trans-[Ru(C≡CC$_6$H$_4$-4-C≡CPh)Cl(dppm)$_2$]	381	101	43	65 ± 40	520 ± 200	520 ± 200
trans-[Ru(C=CHC$_6$H$_4$-4-C≡CPh)Cl(dppm)$_2$]PF$_6$	380	64	31	<500	0	<500
trans-[Ru(C≡CC$_6$H$_4$-4-CHO)Cl(dppm)$_2$]	405	106	38	<120	210 ± 60	210 ± 60
trans-[Ru(C=CHC$_6$H$_4$-4-CHO)Cl(dppm)$_2$]PF$_6$	403	108	39	0	<20	<20
trans-[Ru(C≡CC$_6$H$_4$-4-CHO)Cl(dppe)$_2$]	413	120	40	−300 ± 500	<200	300 ± 500
trans-[Ru(C=CHC$_6$H$_4$-4-CHO)Cl(dppe)$_2$]PF$_6$	412	181	61	<260	0	<260
trans-[Ru(C≡CC$_6$H$_4$-4-NO$_2$)Cl(dppm)$_2$]	473	767	129	170 ± 34[a]	230 ± 46[a]	290 ± 60[a]
trans-[Ru(C=CHC$_6$H$_4$-4-NO$_2$)Cl(dppm)$_2$]PF$_6$	470	721	127	<50	<30	<50
trans-[Ru(C≡CC$_6$H$_4$-4-NO$_2$)Cl(dppe)$_2$]	477	351	55	320 ± 55	<50	320 ± 55
trans-[Ru(C=CHC$_6$H$_4$-4-NO$_2$)Cl(dppe)$_2$]PF$_6$	476	1130	180	250 ± 300	<50	250 ± 300
trans-[Ru(C≡CC$_6$H$_4$-4-C≡CC$_6$H$_4$-4-NO$_2$)Cl(dppm)$_2$]	464	833	161	−160 ± 80	160 ± 60	230 ± 100
trans-[Ru(C=CHC$_6$H$_4$-4-C≡CC$_6$H$_4$-4-NO$_2$)Cl(dppm)$_2$]PF$_6$	326	424	122	<500	420 ± 60	420 ± 60
trans-[Ru(C≡CC$_6$H$_4$-4-(*E*)-CH=CHC$_6$H$_4$-4-NO$_2$)Cl(dppm)$_2$]	490	1964	235	200 ± 40[a]	1100 ± 220[a]	1100 ± 220[a]
trans-[Ru(C=CHC$_6$H$_4$-4-(*E*)-CH=CHC$_6$H$_4$-4-NO$_2$)Cl(dppm)$_2$]PF$_6$	369	1899	314	Scatters	Scatters	Scatters
trans-[Ru(C≡CC$_6$H$_4$-4-(*E*)-CH=CHC$_6$H$_4$-4-NO$_2$)Cl(dppe)$_2$]	489	2676	342	40 ± 200	<100	40 ± 200
trans-[Ru(C=CHC$_6$H$_4$-4-(*E*)-CH=CHC$_6$H$_4$-4-NO$_2$)Cl(dppe)$_2$]PF$_6$	473	441	74	650 ± 500	<50	650 ± 500

[a] CH_2Cl_2 solvent.

tion, into a Langmuir–Blodgett thin film and measured the redox switching of the optical nonlinearity [25]. Switching a three-layer film showed a 50% reduction in second-harmonic generation (SHG) upon oxidation, a significantly smaller decrease than that seen in the molecular measurements. This discrepancy has been attributed to reabsorption of the SHG by the Ru(II) form, together with incomplete oxidation due to poor counter ion migration caused by the insulating alkyl chains.

Redox switching of second-order NLO properties in the ferrocene-based molecules shown in Fig. 4(b) varied from less than a two-fold change in β for the pyridine compound to a 10-fold change in the molybdenum compound with the shortest bridge [26]. Subsequent computational studies on the thiophene-containing compound and its oxidized form using a multiconfigurational reference wavefunction afforded qualitatively similar results [27].

The nitrophenylethenyl ferrocene molecules shown in Fig. 4(c) were attached via the sulfur atom to a gold surface and the electrochemical switching of SHG via these monolayers was investigated [28], oxidation to ferrocenium resulting in a reversible 4- to 5-fold increase in the SHG; while this is a counter-intuitive outcome viewed purely at the molecular level (oxidation converts the molecule from a donor-bridge-acceptor to an acceptor-bridge-acceptor form), the increase in nonlinearity is ascribed by the authors to favourable reorientation at the surface (the molecule is closer to perpendicular after oxidation). Three different redox states of the nonamethylferrocene compound shown in Fig. 4(d) were accessed and their second-order NLO properties were investigated [28]; the central form in Fig. 4(d) has the largest second-order NLO response, which is approximately 10-fold greater than the reduced form, and 20-fold greater than the oxidized form. A fourth state was also demonstrated as a protic switch accessible from the reduced form, but its NLO response was not investigated. Protic switching of quadratic NLO response in coordination complexes has been demonstrated experimentally by Coe et al. [30].

Computational studies have been carried out into the redox switching of the NLO response of the porphyrin compound containing tetrathiafulvalene (TTF) shown in Fig. 5 [31]; a 3.6- and 8.7-fold increase in NLO response of the $TTF^{\bullet+}$ and TTF^{2+} states compared to the ground state being calculated. Calculations were also carried out on the redox switching of the NLO response of some Keggin-type organoimido complexes, a significant change in the NLO response being found between some of the states in the complexes $[PW_{11}O_{39}(ReN)]^{n-}$ ($n = 3$–7) [32] and $[PW_{11}O_{39}(ReNPh)]^{n-}$ ($n = 2$–4) [33], and into the spin crossover switching of the quadratic optical nonlinearity of the iron Schiff base complex shown in Fig. 6 [34], the calculations suggesting that the switching should result in a 25% increase in the response.

5. Metal alkynyl complexes as NLO switches

5.1. Electrochemical switching

The results of single wavelength electrochemical switching of the NLO properties of metal alkynyl complexes are summarized in Table 1, with studies focusing on iron and ruthenium complexes for which reversible $M^{II/III}$ processes are accessible by chemical or electrochemical means. The series of mono-, bi-, and tri-metallic iron alkynyl compounds, shown in Fig. 7, have one to three separately addressable Fe^{II}/Fe^{III} redox events, affording up to four different redox states for $[1,3,5\text{-}C_6H_3\{(C{\equiv}C)Fe(dppe)(\eta^5\text{-}C_5Me_5)\}_3]$, although nonlinearities for the $Fe^{II}/Fe^{II}/Fe^{III}$ and $Fe^{II}/Fe^{III}/Fe^{III}$ forms were equivalent within experimental error [35,36]. The 4-substituted di-iron complex showed a large change in β value, with the mixed valence state $Fe^{II/III}$ having double the value of the $Fe^{II/II}$ and $Fe^{III/III}$ states. In the monometallic iron alkynyl complexes (Fig. 7) [36], the oxidized forms have significantly smaller second-order responses than do the Fe^{II} forms; the largest switching and the largest NLO response are both observed for the 4-nitrophenylethynyl compound, for which the extrapolated zero frequency hyperpolarizability β_0 is 93×10^{-30} esu for the Fe^{II} form and $<1 \times 10^{-30}$ esu for the Fe^{III} form.

Redox switching results in large changes in the third-order nonlinearities of the ruthenium alkynyl compounds shown in Fig. 8, the complexes switching between two-photon absorber (Ru^{II}) and saturable absorber (Ru^{III}) states (Table 1) [37–40]. The trimetallic ruthenium chloride complex shows the largest absolute difference in value, and greatest potential for switching, with

$|\gamma| = 2200 \pm 600 \times 10^{-36}$ esu for Ru^{II} and $14{,}000 \pm 3000 \times 10^{-36}$ esu for Ru^{III}.

Switching the third-order NLO properties of an octupolar iron alkynyl compound (at 695 nm rather than 800 nm as above) has been studied (Fig. 9) [41]. As with its ruthenium alkynyl complex analogue, a change in the sign and magnitude of the two-photon absorption and γ_{imag} values is observed in switching between the Fe$^{II}_3$ and Fe$^{III}_3$ forms, but in contrast to ruthenium, no change in the sign of γ_{real} is seen.

Switching of the third-order NLO properties of the bimetallic iron–ruthenium compound shown in Fig. 10 across three states was effected by selectively oxidizing the iron centre and then the ruthenium centre. At 790 nm, the three states have different NLO absorption, switching from a negligible response in the Fe^{II}Ru^{II} state to a two-photon absorber in the Fe^{III}Ru^{II} state, and then a saturable absorber in the Fe^{III}Ru^{III} state [42].

5.2. *Protic switching*

The second- and third-order NLO properties at a single wavelength of a range of ruthenium alkynyl complexes that can be reversibly switched to the vinylidene form with acid (Fig. 11) have been reported (Table 2) [43]. The quadratic and cubic nonlinearities of many alkynyl/vinylidene complex pairs are similar, the most dramatic differences being a five-fold increase in β and β_0 being observed in proceeding from *trans*-[Ru(C=CHC$_6$H$_4$-4-(*E*)-CH=CHC$_6$H$_4$-4-NO$_2$)Cl(dppe)$_2$]PF$_6$ to *trans*-[Ru(C≡CC$_6$H$_4$-4-(*E*)-CH=CHC$_6$H$_4$-4-NO$_2$)Cl(dppe)$_2$] and a six-fold increase in |γ| being seen in proceeding from *trans*-[Ru(C=CHC$_6$H$_4$-4-NO$_2$)Cl(dppm)$_2$]PF$_6$ to *trans*-[Ru(C≡CC$_6$H$_4$-4-NO$_2$)Cl(dppm)$_2$].

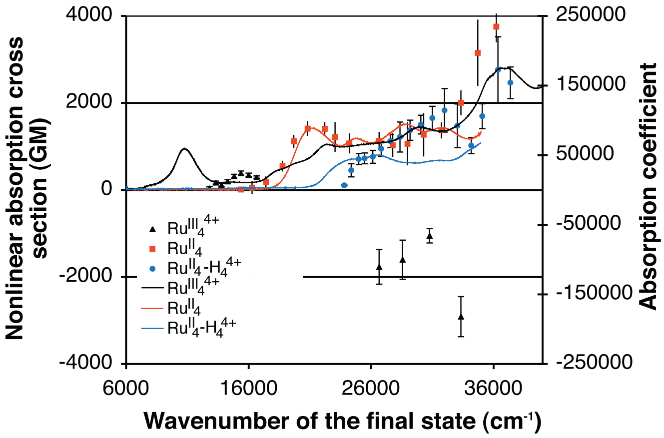

Fig. 13. UV/Vis/NIR and nonlinear absorption spectra of **Ru$^{II}_4$**, **Ru$^{III}_4$**, and **Ru$^{II}_4$–H$_4$$^{4+}$** (see Fig. 12) in CH$_2Cl_2$ [44].

5.3. *Multi-stimuli switching*

The first NLO switching of a metal alkynyl complex using two different stimuli was reported in 2007 [44], concomitant with complete spectral dependence studies, the latter highlighting ideal wavelengths to effect switching. The specific complex possesses a cruciform structure; Fig. 12 shows the protic switch used to interchange between the alkynyl and vinylidene complexes and redox switch used to interchange between the Ru^{II} and Ru^{III} forms, while Fig. 13 displays the wavelength dependence of linear and NLO properties of the three “states”. There are wavelengths at which there are three distinct responses from the three states: a strong two-

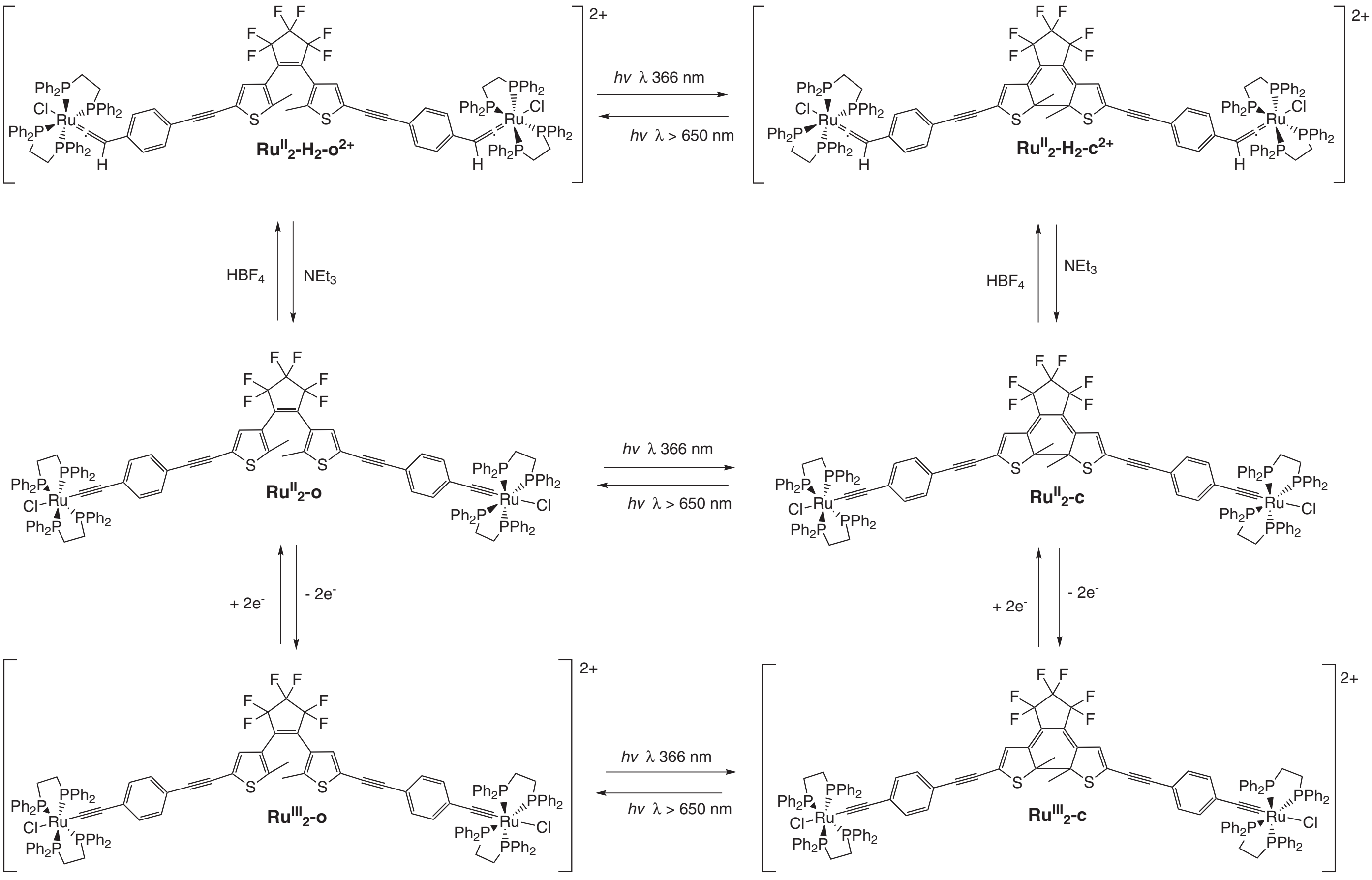

Fig. 14. A ruthenium alkynyl photo-, redox-, and protic switch [45].

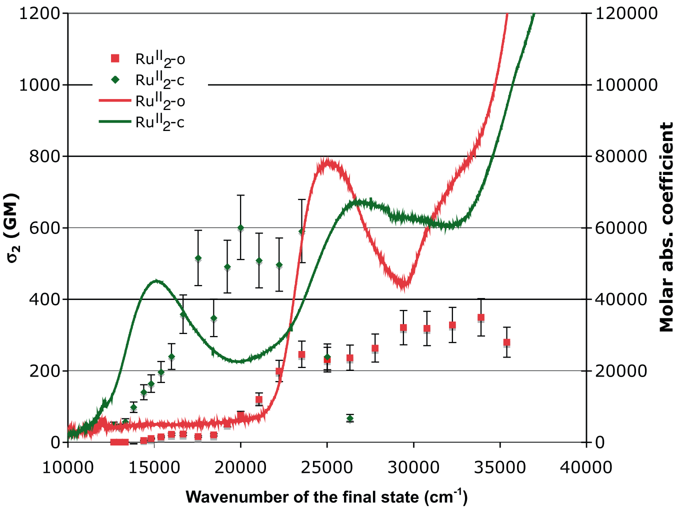

Fig. 15. Linear optical and two-photon absorption spectra for **Ru$^{II}_2$-o** and **Ru$^{II}_2$-c** (see Fig. 14) [45].

photon absorber, a saturable absorber, and negligible nonlinear absorption.

Recently, the electrochemical and protic switching possibilities inherent in a ruthenium alkynyl complex have been combined with a dithienylperfluorocyclopentene photochemical switch to afford a complex with six accessible states that can be inter-converted via seven pathways (Fig. 14) [45]. Each of the six states possesses unique linear and nonlinear optical behavior, and so each of the seven pathways affords the possibility of a "two-state" switch – for an example, see Fig. 15.

6. Concluding remarks

We still await reliable theoretical estimations of nonlinearity (particularly third-order NLO properties), so experimental studies are essential. Initial attempts to effect the switching of nonlinearities were hamstrung by the lack of tuneable light sources – whether a pair of switchable complexes could be used as an NLO switch was frequently due to luck. At the time of our earlier review [3], only NLO data acquired at a single wavelength existed for metal alkynyl complexes and their protic or redox/electrochemical derivatives, and so identifying effective cubic NLO switches, in particular, necessitated collecting data on a large number of switchable pairs and hoping for a positive outcome; while certain guidelines as to the most likely wavelength to effect switching were extant (e.g. probing nonlinear absorption behavior at twice the wavelength of significant one-photon absorption), such studies were still somewhat "hit or miss" in nature. The possibility of acquiring the complete spectral dependence of NLO properties now means that the ideal wavelengths to effect NLO switching for a complex and its switching derivatives are immediately apparent.

The early attempts at NLO switching of metal alkynyl complexes employed one stimulus (usually protonation/deprotonation or oxidation/reduction). It is attractive to think of the oxidation/reduction, protonation/deprotonation, and photoisomerization procedures (the independent switching stimuli) as axes in a 3-dimensional space [46]. One can then increase the number of NLO switching states by proceeding down an axis (e.g., by incorporating iron and ruthenium into a complex (Fig. 10), Fe^{II}Ru^{II}, Fe^{III}Ru^{II} and Fe^{III}Ru^{III} states are available [42]). The alternative to increasing the number of states on one axis is to leave the switching axes. Recent studies have combined these "orthogonal" (independent) stimuli to demonstrate "three-state" switching (in the protonation/deprotonation, oxidation/reduction "plane") [44], and extended these observations by incorporation of photo-switchable modules to demonstrate "six-state" switching (employing all three axes) [45]. The logical steps to further increase the number of NLO states is to incorporate alternative protonation centres into a molecule (responding to a different pH) and addition of new photoisomerizable units responding to different wavelengths of light. The availability of new photo-switchable species that are thermally stable in both states will accelerate this research.

While electrochemical switching of the nonlinearity of metal alkynyl complexes has thus far been carried out only in solution, with a resultant ca. 10–20 min switching cycle, there are prospects for success with the goal of much-more-rapid switching; a 4-ethynylphenylethynyl-functionalized derivative of the iron-ruthenium complex in Fig. 10 has been attached to a conducting silicon surface via a hydrosilylation procedure, the resultant nanostructure undergoing stepwise oxidation. The oxidation was monitored by cyclic voltammetry, with the resultant cyclic voltammogram being analogous to that of the complexes in solution [47]. Despite this success, "instantaneous" surface-supported NLO switching of metal alkynyl complexes still necessitates assembling a sufficient number density of molecules at a surface for observable effects. Increasing control over surface-supported nanoarchitectures will accelerate this research.

Acknowledgements

We thank the Commonwealth of Australia for an Australian Postgraduate Award (K.A.G.), the Australian Research Council for an ARC Australian Professorial Fellowship (M.G.H.) and an ARC Australian Research Fellowship (M.P.C.), and the Foundation for Polish Science for the award of a Welcome Programme Laureateship (M.S.).

References

[1] For selected reviews, see:
(a) D.J. Williams, Angew. Chem. Int. Ed. 23 (1984) 690;
(b) S.R. Marder, J.E. Sohn, G.D. Stucky (Eds.), Materials for Nonlinear Optics, Chemical Perspectives, American Chemical Society, Washington, DC, 1991;
(c) B. Kirtman, B. Champagne, Int. Rev. Phys. Chem. 16 (1997) 389;
(d) M.G. Papadopoulos, A.J. Sadlej, J. Leszczynski (Eds.), Non-Linear Optical Properties of Matter: From Molecules to Condensed Phases, Springer, Dordrecht, The Netherlands, 2006;
(e) G.S. He, L.-S. Tan, Q. Zheng, P.N. Prasad, Chem. Rev. 108 (2008) 1245;
(f) D.N. Christodoulides, I.C. Khoo, G.J. Salamo, G.I. Stegeman, E.W. Van Stryland, Adv. Opt. Photon. 2 (2010) 60.
[2] For selected reviews, see:
(a) H.S. Nalwa, Appl. Organomet. Chem. 5 (1991) 1;
(b) S.R. Marder, in: D.W. Bruce, D. O'Hare (Eds.), Inorganic Materials, Wiley, Chichester, 1992, p. 116;
(c) H. Nalwa, Adv. Mater. 5 (1993) 341;
(d) D.R. Kanis, M.A. Ratner, T.J. Marks, Chem. Rev. 94 (1994) 195;
(e) N.J. Long, Angew. Chem. Int. Ed. 34 (1995) 21;
(f) T. Verbiest, S. Houbrechts, M. Kauranen, K. Clays, A. Persoons, J. Mater. Chem. 7 (1997) 2175;
(g) I.R. Whittall, A.M. McDonagh, M.G. Humphrey, M. Samoc, Adv. Organomet. Chem. 42 (1998) 291;
(h) I.R. Whittall, A.M. McDonagh, M.G. Humphrey, M. Samoc, Adv. Organomet. Chem. 43 (1999) 349;
(i) D.M. Roundhill, J.P. Fackler, Optoelectronic Properties of Inorganic Compounds, Plenum, New York, 1999;
(j) S. Di Bella, Chem. Soc. Rev. 30 (2001) 355;
(k) E. Cariati, M. Pizzotti, D. Roberto, F. Tessore, R. Ugo, Coord. Chem. Rev. 250 (2006) 1210;
(l) J.P.L. Morrall, M.G. Humphrey, G.T. Dalton, M.P. Cifuentes, M. Samoc, in: M.G. Papadopoulos, A.J. Sadlej, J. Leszczynski (Eds.), Non-Linear Optical Properties of Matter: From Molecules to Condensed Phases, Springer, Dordrecht, The Netherlands, 2006, p. 537;
(m) C. Zhang, Y. Song, X. Wang, Coord. Chem. Rev. 251 (2007) 111;
(n) J.P. Morrall, G.T. Dalton, M.G. Humphrey, M. Samoc, Adv. Organomet. Chem. 55 (2008) 61;
(o) S. Di Bella, C. Dragonetti, M. Pizzotti, D. Roberto, F. Tessore, R. Ugo, Top. Organomet. Chem. 28 (2010) 1;
(p) M.G. Humphrey, M.P. Cifuentes, M. Samoc, Top. Organomet. Chem. 28 (2010) 57.

[3] C.E. Powell, M.G. Humphrey, Coord. Chem. Rev. 248 (2004) 725.
[4] R.W. Boyd, Nonlinear Optics, Academic Press, New York, 1992.
[5] B.L. Feringa, Molecular Switches, Wiley, Weinheim, 2001.
[6] For selected reviews, see:
(a) B.J. Coe, Chem.-Eur. J. 5 (1999) 2464;
(b) G. Berkovic, V. Krongauz, V. Weiss, Chem. Rev. 100 (2000) 1741;
(c) B.L. Feringa, R.A. van Delden, N. Koumura, E.M. Geertsema, Chem. Rev. 100 (2000) 1789;
(d) N. Hampp, Chem. Rev. 100 (2000) 1755;
(e) M. Irie, Chem. Rev. 100 (2000) 1685;
(f) Y. Yokoyama, Chem. Rev. 100 (2000) 1717;
(g) B.J. Coe, in: M.G. Papadopoulos, A.J. Sadlej, J. Leszczynski (Eds.), Non-Linear Optical Properties of Matter: From Molecules to Condensed Phases, Springer, Dordrecht, The Netherlands, 2006, p. 571;
(h) V. Guerchais, H. Le Bozec, Top. Organomet. Chem. 28 (2010) 171;
(i) V. Guerchais, L. Ordonneau, H. Le Bozec, Coord. Chem. Rev. 254 (2010) 2533;
(j) H. Nakai, K. Isobe, Coord. Chem. Rev. 254 (2010) 2652.
[7] See, for example:
(a) K. Szaciłowski, Chem. Rev. 108 (2008) 3481;
(b) A. Bousseksou, G. Molnár, J.A. Real, K. Tanaka, Coord. Chem. Rev. 251 (2007) 1822;
(c) V. Balzani, A. Credi, S. Silvi, M. Venturi, Chem. Soc. Rev. 35 (2006) 1135.
[8] (a) B.L. Feringa, Acc. Chem. Res. 34 (2001) 504;
(b) B.L. Feringa, N. Koumura, R.A. van Delden, M.K.J. Ter Wiel, Appl. Phys. A 75 (2002) 301.
[9] (a) D. Baylor, Proc. Natl. Acad. Sci. U.S.A. 93 (1996) 560;
(b) P.C. Pandey, Anal. Chim. Acta 568 (2006) 47;
(c) G. Chen, X. Shang, G. Yang, Z. Hao, X. Xu, C. Zhang, Q.W. Song, Optik 120 (2009) 721;
(d) R.A. Mathies, S.W. Lin, J.B. Ames, W.T. Pollard, Annu. Rev. Biophys. Biophys. Chem. 20 (1991) 491.
[10] J. Daub, T. Knöchel, A. Mannschreck, Angew. Chem. Int. Ed. 23 (1984) 960.
[11] (a) V. De Waele, U. Schmidhammer, T. Mrozek, J. Daub, E. Riedle, J. Am. Chem. Soc. 124 (2002) 2438;
(b) L. Gobbi, P. Seiler, F. Diederich, V. Gramlich, C. Boudon, J.P. Gisselbrecht, M. Gross, Helv. Chim. Acta 84 (2001) 743.
[12] (a) M. Tomasulo, S. Sortino, A.J.P. White, F.M. Raymo, J. Org. Chem. 70 (2005) 8180;
(b) M. Tomasulo, S. Sortino, F.M. Raymo, Org. Lett. 7 (2005) 1109.
[13] A.S. Dvornikov, P.M. Rentzepis, Mol. Cryst. Liq. Cryst. 246 (1994) 379.
[14] (a) E. Zahavy, S. Rubin, I. Willner, J. Chem. Soc. Chem. Commun. (1993) 1753;
(b) E. Zahavy, S. Rubin, I. Willner, Mol. Cryst. Liq. Cryst. 246 (1994) 195.
[15] S. Jockusch, N. Turro, F.R. Blackburn, J. Phys. Chem. A 106 (2002) 9236.
[16] (a) I. Calderara, U.S. Patents 6,224,945 (1997).;
(b) B. Van Germert, U.S. Patents 5,645,767 (1997).
[17] M.A.L. Sheepwash, R.H. Mitchell, C. Bohne, J. Am. Chem. Soc. 124 (2002) 4693.
[18] K. Matsuda, M. Irie, J. Photochem. Photobiol. C 5 (2004) 169.
[19] (a) L. Fabbrizzi, M. Licchelli, G. Rabaioli, A. Taglietti, Coord. Chem. Rev. 205 (2000) 85;
(b) J.F. Callan, A.P. de Silva, D.C. Magri, Tetrahedron 61 (2005) 8551;
(c) A. Robertson, S. Shinkai, Coord. Chem. Rev. 205 (2000) 157.
[20] I. Asselberghs, Y. Zhao, K. Clays, A. Persoons, A. Comito, Y. Rubin, Chem. Phys. Lett. 364 (2002) 279.
[21] (a) T. Nagamura, H. Sakaguchi, T. Matsuo, Thin Solid Films 210 (1992) 160;
(b) H. Sakaguchi, L.A. Gomez-Jahn, M. Prichard, T.L. Penner, J. Phys. Chem. 97 (1993) 1474;
(c) H. Sakaguchi, T. Nagamura, T.L. Penner, D.G. Whitten, Thin Solid Films 244 (1994) 947.
[22] F.Z. Henari, J. Opt. A: Pure Appl. Opt. 3 (2001) 188.
[23] K. Meerholz, J. Swiatkiewicz, P.N. Prasad, J. Phys. Chem. 99 (1995) 7715.
[24] B.J. Coe, S. Houbrechts, I. Asselberghs, A. Persoons, Angew. Chem. Int. Ed. 38 (1999) 366.
[25] L. Boubekeur-Lecaque, B.J. Coe, K. Clays, S. Foerier, T. Verbiest, I. Asselberghs, J. Am. Chem. Soc. 130 (2008) 3286.
[26] (a) M. Malaun, Z.R. Reeves, R.L. Paul, J.C. Jeffery, J.A. McCleverty, M.D. Ward, I. Asselberghs, K. Clays, A. Persoons, Chem. Commun. (2001) 49;
(b) M. Malaun, R. Kowallick, A.M. McDonagh, M. Marcaccio, R.L. Paul, I. Asselberghs, K. Clays, A. Persoons, B. Bildstein, C. Fiorini, J.M. Nunzi, M.D. Ward, J.A. McCleverty, J. Chem. Soc. Dalton Trans. (2001) 3025;
(c) I. Asselberghs, K. Clays, A. Persoons, A.M. McDonagh, M.D. Ward, J.A. McCleverty, Chem. Phys. Lett. 368 (2003) 408.
[27] H. Reis, M.G. Papadopoulos, PCCP 5 (2003) 1190.
[28] T. Kondo, S. Horiuchi, I. Yagi, S. Ye, K. Uosaki, J. Am. Chem. Soc. 121 (1999) 391.
[29] C. Sporer, I. Ratera, D. Ruiz-Molina, Y. Zhao, J. Vidal-Gancedo, K. Wurst, P. Jaitner, K. Clays, A. Persoons, C. Rovira, J. Veciana, Angew. Chem. Int. Ed. 43 (2004) 5266.
[30] B.J. Coe, J.L. Harries, M. Helliwell, L.A. Jones, I. Asselberghs, K. Clays, B.S. Brunschwig, J.A. Harris, J. Garin, J. Orduna, J. Am. Chem. Soc. 128 (2006) 12192.
[31] C.G. Liu, W. Guan, P. Song, L.K. Yan, Z.M. Su, Inorg. Chem. 48 (2009) 6548.
[32] W. Guan, G. Yang, C. Liu, P. Song, L. Fang, L. Yan, Z. Su, Inorg. Chem. 47 (2008) 5245.
[33] W. Guan, C.G. Liu, P. Song, G.C. Yang, Z.M. Su, Theor. Chem. Acc. 122 (2009) 265.
[34] F. Averseng, C. Lepetit, P.G. Lacroix, P.J. Tuchagues, Chem. Mater. 12 (2000) 2225.
[35] T. Weyland, I. Ledoux, S. Brasselet, J. Zyss, C. Lapinte, Organometallics 19 (2000) 5235.
[36] F. Paul, K. Costuas, I. Ledoux, S. Deveau, J. Zyss, J.F. Halet, C. Lapinte, Organometallics 21 (2002) 5229.
[37] M.P. Cifuentes, C.E. Powell, M.G. Humphrey, G.A. Heath, M. Samoc, B. Luther-Davies, J. Phys. Chem. A 105 (2001) 9625.
[38] C.E. Powell, M.P. Cifuentes, J.P. Morrall, R. Stranger, M.G. Humphrey, M. Samoc, B. Luther-Davies, G.A. Heath, J. Am. Chem. Soc. 125 (2003) 602.
[39] C.E. Powell, M.G. Humphrey, M.P. Cifuentes, J.P. Morrall, M. Samoc, B. Luther-Davies, J. Phys. Chem. A 107 (2003) 11264.
[40] M.P. Cifuentes, C.E. Powell, J.P. Morrall, A.M. McDonagh, N.T. Lucas, M.G. Humphrey, M. Samoc, S. Houbrechts, I. Asselberghs, K. Clays, A. Persoons, T. Isoshima, J. Am. Chem. Soc. 128 (2006) 10819.
[41] M.P. Cifuentes, M.G. Humphrey, J.P. Morrall, M. Samoc, F. Paul, C. Lapinte, T. Roisnel, Organometallics 24 (2005) 4280.
[42] M. Samoc, N. Gauthier, M.P. Cifuentes, F. Paul, C. Lapinte, M.G. Humphrey, Angew. Chem. Int. Ed. 45 (2006) 7376.
[43] S.K. Hurst, M.P. Cifuentes, J.P. Morrall, N.T. Lucas, I.R. Whittall, M.G. Humphrey, I. Asselberghs, A. Persoons, M. Samoc, B. Luther-Davies, A.C. Willis, Organometallics 20 (2001) 4664.
[44] G.T. Dalton, M.P. Cifuentes, S. Petrie, R. Stranger, M.G. Humphrey, M. Samoc, J. Am. Chem. Soc. 129 (2007) 11882.
[45] K.A. Green, M.P. Cifuentes, T.C. Corkery, M. Samoc, M.G. Humphrey, Angew. Chem. Int. Ed. 48 (2009) 7870.
[46] A similar visualization of six-state molecular switching of linear optical properties is described in: L. Gobbi, P. Seiler, F. Diederich, Angew. Chem. Int. Ed. 38 (1999) 674.
[47] N. Gauthier, G. Argouarch, F. Paul, M.G. Humphrey, L. Toupet, S. Ababou-Girard, H. Sabbah, P. Hapiot, B. Fabre, Adv. Mater. 20 (2008) 1952.